# Immiscible displacement of viscosity-matched fluids in two-dimensional porous media

Olav Inge Frette, Knut Jørgen Måløy, and Jean Schmittbuhl*
*Fysisk Institutt, Universitetet i Oslo, P.O. Box 1048, Blindern, N-0316, Oslo 3, Norway*

Alex Hansen
*Institutt for Fysikk, Norges Teknisk-Naturvitenskapelige Universitet, N-7034 Trondheim, Norway*
(Received 15 May 1996; revised manuscript received 17 September 1996)

The effect of stabilization has been investigated experimentally when a nonwetting fluid is displacing a wetting fluid with the same viscosity in a two-dimensional porous medium. Experiments were done at different injection rates, with capillary numbers ranging from $10^{-7}$ to $10^{-4}$. The features of the front between the liquids were analyzed and found similar to those observed from invasion percolation models including a spatial gradient in the average pore threshold value, and gravitationally stabilized experiments. Front and structure of the trapped clusters of the invaded fluid at different capillary numbers are self-similar with the fractal dimensions $D_b = 1.33$ and $D_b^m = 1.85$, respectively. The dependence of the front width $w_s$ on the capillary $C_a$ was found to be consistent with a power law $w_s \sim C_a^{-\alpha}$, with $\alpha = 0.6$. The dynamic exponent $\beta_d \approx 0.8$ describing front width evolution as a function of time was determined by collapsing the density-density correlation function data. An analytical argument is presented to support the stabilization of the front owing to the viscous effects. [S1063-651X(96)05012-X]

PACS number(s): 47.55.Mh, 05.40.+j, 47.55.Kf

## I. INTRODUCTION

The structure and dynamics of two-phase flow in porous media have been the object of a large number of studies in recent years. One of the main reasons for this is the rich variety of structures which can be created depending on the relative viscosity, interface tension, wettability, and displacement rate [1–6]. Two-phase flow in a porous medium is also of large practical importance in secondary oil recovery. In this paper we restrict the discussion to drainage in two-dimensional systems, i.e., the process where a nonwetting fluid displaces a wetting fluid in a porous medium. In the limit of very slow injection rates, the displacement process depends entirely on the capillary pressure threshold fluctuations at the pore level [7–9]. In this limit, the pressure drop due to the viscous flow field can be neglected. However, the presence of a gravity field may either stabilize [10] or destabilize the front [11,12]. At slow injection rates, it is observed experimentally that the front movement is not continuous, but occurs in sudden bursts, called Haines jumps [13]. Recent theoretical studies [14–18] and experiments [16,18] have revealed general scaling features of the burst dynamics in slow drainage. In the limit of high injection rates, the structures observed depend critically on the viscosity ratio of the fluids [3]. When the injected fluid has a lower viscosity than the displaced fluid, the situation is highly unstable and ramified viscous fingers are observed [1,2,19,20]. In the opposite case when the injected liquid has a higher viscosity, the situation is stable [3], and the front reaches a steady width.

We report on the experimental study of drainage in a two-dimensional porous model with liquids which have the same viscosity. The front is found to stabilize (i.e., flatten) at large displacement rates. We emphasize that the velocity field in our experiments is not homogeneous. The mechanism that stabilizes the front is different from that of experiments with a gravitational field which is homogeneous. In the latter case, the front propagation may be mapped onto an invasion percolation process with a gradient in the average pore threshold value [10,21,22] and the competition between the gravitational and capillary forces is described by the bond number, $B_0 = g a^2 \delta\rho / \gamma$, where $g$ is the gravitational constant, $a$ is a typical pore size, $\gamma$ is the interface tension, and $\delta\rho$ the density difference between the liquids. The bond number gives the strength of the external field which corresponds to the gradient used in the invasion percolation simulation. Recent experiments and simulations show an excellent agreement with this mapping first suggested by Wilkinson [21]. However, this analysis is not suited for the case we study here, where the pressure gradient is dominated by viscous flow. The trapped clusters and the pore size fluctuations give rise in this case to significant pressure fluctuations that cannot be neglected.

Wilkinson also went further with a theoretical approach to the viscous problem in three dimensions [21,22]. By using the Darcy law, the concept of relative permeability, and a percolation approach for the saturation of the nonwetting fluid, he proposed the scaling relation $w_s \sim C_a^{-\nu/(t+1-\beta+\nu)}$ for the width of the front. Here $\nu$ is the correlation length exponent, $\beta$ is the order parameter exponent, and $t$ is the conductivity exponent in percolation. The capillary number is the ratio between the viscous and the capillary forces and is defined as $C_a = \mu v / \gamma$, where $\mu$ is the dynamic viscosity, $v$ is the superficial velocity, i.e., volume flux, and $\gamma$ is the interface tension. However, we emphasize that this theory is not necessarily valid in two dimensions, because of the importance of trapping of the displaced fluid. In three dimensions, trapping may be neglected. By using the Darcy law,

*Permanent address: Laboratorie de Géologie, Ecole Normale Supérieure, 24 rue Lhomond, F-75 231 Paris Cedex 05, France.

 

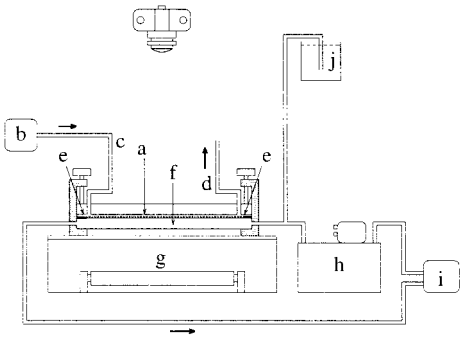


FIG. 1. The experimental setup. (a) Plexiglas beads, (b) precision pump with constant flow rate, (c) inlet, (d) outlet, (e) thermistors, (f) mylar membrane and pressure pillow filled with water, (g) light case, (h) Hetro regulator, (i) pump, (j) water pressure source.

this theory is also a mean field approach, neglecting fluctuations in the velocity field. To our knowledge, no experiments have been performed that test this scaling relation in three dimensions. In the theory of Wilkinson, it is assumed that the viscosity of the injected fluid is higher than that of the displaced fluid. This is not the case in the experiments we report on here, where the viscosities of the two liquids are equal. However, as will be argued in the following, trapping and flow in local capillary fingers induce a decrease in effective permeability of the invaded regions, which may be interpreted as an increase of effective viscosity of the invading fluid. Thus, this condition for the Wilkinson theory to apply is fulfilled.

We performed experiments in two-dimensional porous media at different displacement rates. The dependence of the saturated front width $w_s$ on the capillary number $C_a$ was measured and found consistent with a power law $w_s \sim C_a^{-\alpha}$ with $\alpha = 0.6$. The front itself is found to be fractal with a fractal dimension equal to $D_b = 1.33$, consistent with the fractal dimension of the external perimeter in invasion percolation and results obtained from gravitational stabilized fluid fronts. The distribution function of the trapped clusters, generated by the front, was also found to be consistent with invasion percolation results. The dynamics of the front was investigated by measuring the dynamic exponent $\beta_d$, describing the time dependence of the front width.

The paper is structured as follows: in Sec. II, we describe the experiments, in Sec. III we present the experimental results, and in Sec. IV we discuss and compare the results to those of other studies.

## II. EXPERIMENTS

The experimental setup is shown in Fig. 1. The porous model consists of a monolayer of Plexiglas beads of diameter $d = 0.7$ mm, randomly spread between two contact papers [1]. The model is transparent and has a porosity $\phi = 0.7$. A rectangular silicon rubber packing provides boundary of the model of size 350 mm $\times$ 350 mm.

A 2 cm thick glass plate is placed on the top and clamped together with a 2 cm Plexiglas plate lying underneath the model. Both rigid plates prevent bending of the model. In the middle, the layer of Plexiglas beads is glued between the contact papers. To squeeze the beads and the contact paper together with the upper plate, a mylar membrane, below the model, is kept under a 2.5 m water pressure provided by an external reservoir connected to the model. To prevent gravitational effects, the upper glass plate is carefully leveled to within 0.1 mm.

Since the viscosity of the liquids is sensitive to temperature variations, it is important to control the temperature inside the model. This is done by circulating water in the mylar pillow through a controlled temperature bath. The temperature is measured inside the model by two thermistors mounted close to the inlet and the outlet of the porous model. With this temperature regulator, the temperature difference between the two sides of the model is kept within 0.1 K for all experiments. The temperature drift during time was less than 0.1 K for the fast experiments (shorter than 5 h) and about 0.3 K for the slowest experiment (150 h). It is important to note that the temperature drift for slow experiments is not important since the viscous pressure gradients are negligible compared to the capillary ones.

The model was initially filled with a hexamethyldisiloxane silicone oil. The displacing fluid is a 20% (by weight) water glycerol solution with 0.2% nigrosine dye. The temperature dependence of the viscosity of each fluid has been measured and used to estimate the temperature at which viscosity matching is achieved. These measurements were performed with the same thermistors as the ones used in the model. This suppresses zero point shift of the temperature. The temperature of equal dynamic viscosity ($\mu = 47.8$ cP) is 24.5 °C.

The interface tension between both liquids is measured by using a pendant drop method [23] giving $\gamma = 28$ dyn/cm. Experiments were performed to check the wetting properties of the fluids by using droplets of the water-glycerol mixture immersed in the silicon oil on a substrate of Plexiglas and contact paper. We found that silicon oil wets both Plexiglas and contact paper with an almost equal wetting angle: $\alpha \approx 50°$ (i.e., the angle between the substrate and the water-glycerol droplet).

The displacement process is visualized by illuminating the model from below and pictures are taken from above with a Kodak DCS 420 CCD camera. The images have a resolution of $1536 \times 1024$ pixels and are analyzed by using an image processing software specifically developed for this purpose. An example of a high resolution photograph of a fully developed drainage front at a capillary number $C_a = 4.40 \times 10^{-7}$ is shown in Fig. 2. The spatial resolution is 0.2 mm per pixel. The nonwetting fluid is shown as black and moves downwards in the image. A complicated fractal front is observed with trapped clusters behind the front. The grey level distribution of the image presents two peaks which correspond, respectively, to the white and the dark parts of the image. The image is clipped with a threshold set at the minimum between the peaks. Cluster size distributions are calculated from the clipped image. The drainage front is extracted as the boundary of the largest cluster of the image. Figure 2(b) shows the front between fluids of Fig. 2(a).

## III. EXPERIMENTAL RESULTS

Experiments at different injection rates were performed to study the dependence of the front geometry on the capillary

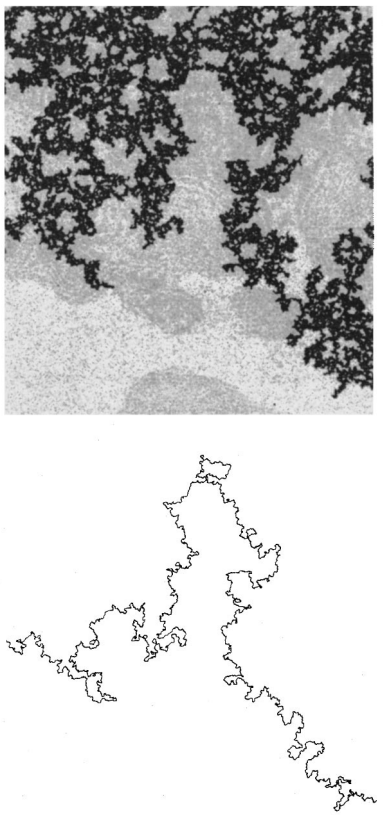

FIG. 2. (a) Displacement structure observed at $C_a = 4.40\times10^{-7}$. The dimension of the image is 350 mm$\times$ 350 mm. (b) The extracted fluid front of the structure in (a).

number $C_a$. The injection rates and the capillary number used in the different experiments are given in Table I. Examples of six different experiments at different injection rates are shown in Fig. 3. At low injection rates, the structure resembles the structures observed in invasion percolation. At increased injection rate, the front stabilizes. As will be discussed below, the trapping and the movement in local capillary fingers are essential to get a stable front when the viscosity ratio is equal to 1.

To calculate the front width $w$, we counted the number $n(y)$ of pixels belonging to the front, at constant distance $y$ from the average position of the front. The distribution $n(y)$ is found to be roughly Gaussian. The front width $w$ is defined as a standard deviation of $n(y)$. We assume that the front width $w$ follows the scaling relation:

$$w = t^{\beta_d} h(t, C_a). \tag{1}$$

The first term, $t^{\beta_d}$, describes the time dependence of the front width. However, the viscous pressure gradients in the fluids stabilize the front and introduce a length scale in the system at large times $t$. This length scale is identified as the saturation width $w_s$ of the front. At short time scales, $t \ll w_s^{1/\beta_d}$, the crossover function $h(t,C_a)$ is independent of time $t$: $h(t,C_a) = c(C_a)$. At large time scales, $t \gg w_s^{1/\beta_d}$, the crossover function $h(t,C_a)$ has the form $t^{-\beta_d} w_s(C_a)$, where $w_s$ is only a function of the capillary number $C_a$.

When the front develops, it reaches a saturated front width $w_s$. Figure 4 shows $w_s$ as a function of the capillary number. It is possible that the slowest experiment ($C_a = 4.40\times10^{-7}$) has not reached saturation, due to the limited size of our model. As a consequence the saturation width of the slowest experiment may be underestimated in contrast to the other experiments. Assuming a power law dependence of the saturated front width on the capillary number $w_s \sim C_a^{-\alpha}$ we found an exponent $\alpha = 0.6 \pm 0.2$. In three dimensions Wilkinson has proposed the scaling relation [21] $w_s \sim C_a^{-\nu/(t+1-\beta+\nu)}$ However, we will emphasize that this theory is valid in three dimensions. Using the exponents from two-dimensional percolation in this relation gives $\alpha = 0.38$.

The fractal structures of the fronts are characterized by using the box counting algorithm and the density-density correlation function. In the box counting procedure, the number of boxes with size $\delta$ needed to cover the front scales as

$$N(\delta) = N_0 w^{-D_b} f\left(\frac{\delta}{w}\right), \tag{2}$$

where $D_b$ is the box counting dimension, and $N_0$ is the number of boxes of size $\delta = 1$. Here the lengths are measured in units of the average pore size $a \approx 0.7$ mm. The box counting dimension was found by fitting the scaling function $f(x)$ to the functional form $f(x) \propto x^{-D_b}$. This is obtained by searching the linear fit of $\log(N(\delta) w^{D_b}/N_0) = -D_b \log(\delta/w) + A$, with $D_b$ and $A$ as the free parameters. Figure 5 shows the data collapse, for all experiments. The fractal dimension is estimated as $D_b = 1.33 \pm 0.05$. The data are fitted in the range $1/w < \delta/w < 1$. When $\delta > w$, the front is seen as a one-dimensional object with a slope equal to 1.

The second method to determine the fractal dimension of the fronts is to compute the density-density correlation function, see, e.g., Gouyet *et al.* [24]. The density-density correlation function is

$$C(r) = \langle\langle \rho(\vec{r}_0)\rho(\vec{r}_0+\vec{r})\rangle\rangle_{|\vec{r}|=r}. \tag{3}$$

Here $\vec{r}_0$ is a particular position on the front, and $\vec{r}$ is a vector from this point. $\rho(\vec{r}_0)$ is the grey level density of the pixel located at $\vec{r}_0$. The double average reflects an averaging over all possible positions $\vec{r}_0$, and over all possible directions of

TABLE I. The values of the flow rate, velocity, and capillary number and front width for the 11 experiments.

| Flow rate ($cm^3$/h) | Superficial velocity (cm/h) | $C_a$ | $w_s$ (Units of pore size) |
|---|---|---|---|
| 133 | 67.9 | $3.32\times10^{-4}$ | 2.69 |
| 13.6 | 6.91 | $3.38\times10^{-5}$ | 5.96 |
| 8.56 | 4.37 | $2.14\times10^{-5}$ | 6.84 |
| 5.61 | 2.86 | $1.40\times10^{-5}$ | 6.49 |
| 2.81 | 1.44 | $7.03\times10^{-6}$ | 8.56 |
| 1.91 | 0.972 | $4.76\times10^{-6}$ | 13.4 |
| 1.16 | 0.593 | $2.90\times10^{-6}$ | 19.5 |
| 0.850 | 0.433 | $2.12\times10^{-6}$ | 24.0 |
| 0.536 | 0.273 | $1.34\times10^{-6}$ | 22.0 |
| 0.416 | 0.212 | $1.04\times10^{-6}$ | 46.4 |
| 0.176 | 0.0896 | $4.40\times10^{-7}$ | 60 |

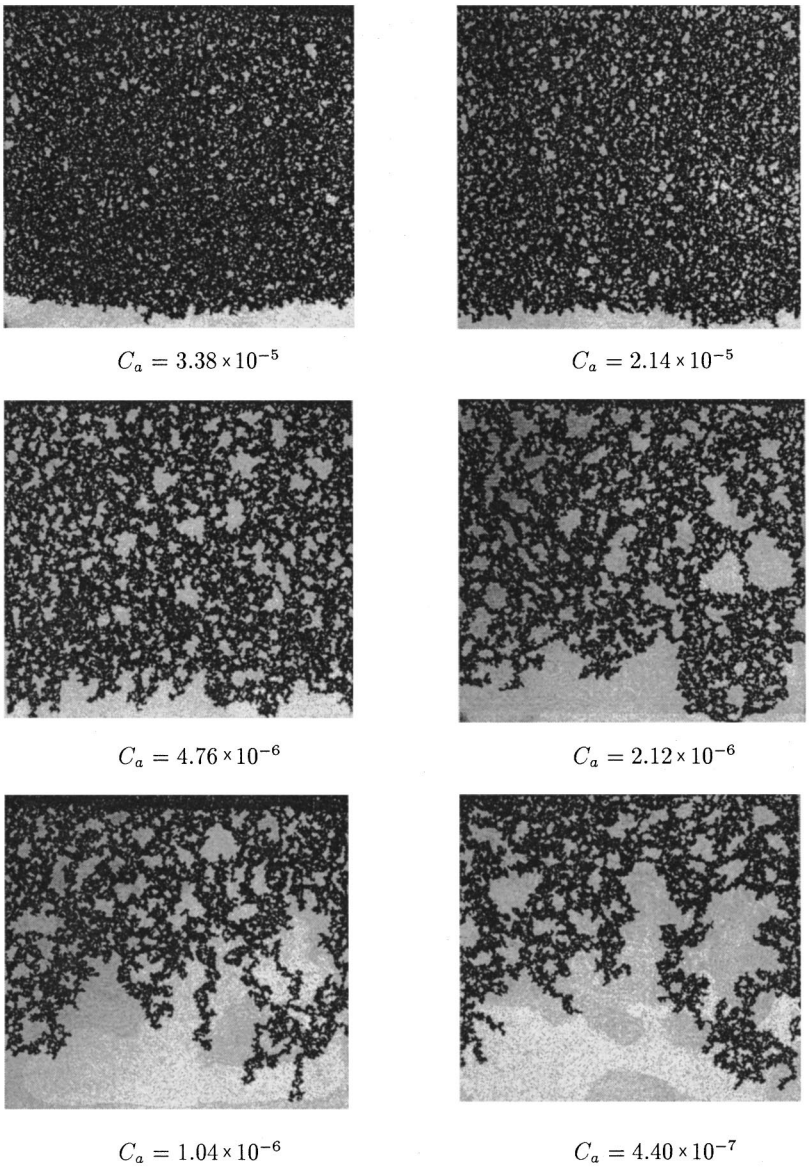


FIG. 3. The structure of six different experiments near breakthrough. The dimension of the image is 350 mm × 350 mm. The experiment at $C_a = 3.38 \times 10^{-5}$ shows a compact structure, narrow front, and small trapped clusters. The experiment at $C_a = 4.40 \times 10^{-7}$ shows a very wide front with trapped clusters on many length scales.

$\vec{r}$. For a self-similar fractal, the density-density correlation function is expected to scale as

$$C(r) = w^{-\alpha} g\left(\frac{r}{w}\right), \tag{4}$$

where $w$ is the width of the front. The function $g(x)$ behaves as $g(x) \sim x^{-\alpha}$ for $x \ll 1$ and $g(x) \sim x^{-1}$ for $x \gg 1$. The exponent $\alpha$ verifies the relation $\alpha = 2 - D_d$, where $D_d$ is the fractal dimension. In Fig. 6, the scaling function is fitted with $\alpha = 0.58 \pm 0.05$ or $D_d = 1.42 \pm 0.05$. The fitting of the data was done for length scales larger than the pore size and smaller than the width of the front ($r/w \ll 1$). The fractal dimension is consistent with that obtained from box counting ($D_b = 1.33$). We want to emphasize that these results are found by a data collapse of both slow and fast experiments, and that the local structure of the fast experiments within the front width seems similar to the structure obtained at very slow injection rates. Moreover, both fractal dimensions $D_b$ and $D_d$ are close to the fractal dimension of the external perimeter of invasion percolation cluster, which is $D_e = 4/3$ [25,26]. The result is also consistent with the result obtained for gravitational stabilized drainage fronts [10].

By using Eqs. (1) and (4), and assuming that $t \ll w_s^{1/\beta_d}$, we find

$$C(r) = w^{-\alpha} g\left(\frac{r}{ct^{\beta_d}}\right) = r^{-\alpha} G\left(\frac{r}{ct^{\beta_d}}\right), \tag{5}$$

where $G(x)$ is constant for $x \ll 1$ and $G(x) \sim x^{\alpha - 1}$ for $x \gg 1$. In Fig. 7, we plot $C(r) r^{\alpha}$ as a function of $r/(ct^{\beta_d})$ by choosing the value of $\beta_d$, which gave the best data collapse. It is difficult to get a very precise value of the dynamic exponent $\beta_d$, due to the limited size of our models. Assuming a power law behavior, the best estimate for $\beta_d$ obtained on the basis of experiments performed at different capillary numbers is $\beta_d = 0.8 \pm 0.3$.

The fractal structure of the mass of the displacing fluid is also studied by using the box counting procedure. We show in Fig. 8 the box counting data for three experiments in a log-log plot. By fitting the data we found a fractal dimension $D_b^m = 1.85 \pm 0.07$. Again this result is consistent with the frac-

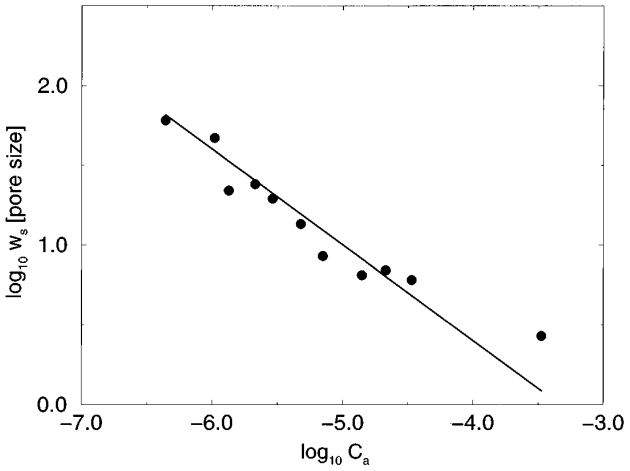


FIG. 4. The front width $w_s$ as a function of the capillary number $C_a$. $w_s$ is measured in units of average pore size. The solid line has a slope of 0.6.

tal dimension of invasion percolation clusters with trapping [8] and experiments of very slow drainage in a two-dimensional porous medium [9].

The structure of the invading fluid is generated by the front, and therefore the length of the trapped clusters should scale as the width of the front (trapped clusters are clusters of the displaced fluid trapped in the invading fluid). The size distribution of the trapped clusters was measured for the different flow rates. In Fig. 9, the cumulative distribution of the trapped clusters is plotted as function of the cluster size in a log-log plot for six experiments with different injection rates. This distribution is expected to scale like $N(s) = s^{-\tau+1} N_1 f(s/s_{\max})$, where $s_{\max}$ is the size of the largest trapped cluster and $N_1 = N \ (s=1)$. The slope of the cumulative cluster distribution for the slowest displacement rate was found to be $-0.70 \pm 0.10$, which gives $\tau = 1.70 \pm 0.10$. Scaling arguments given by Meakin [28] predict a scaling relation which in two dimensions is

$$\tau = 1 + \frac{D}{2}, \tag{6}$$

between the cluster distribution exponent $\tau$ and the fractal dimension $D$ of the structure itself. For invasion percolation

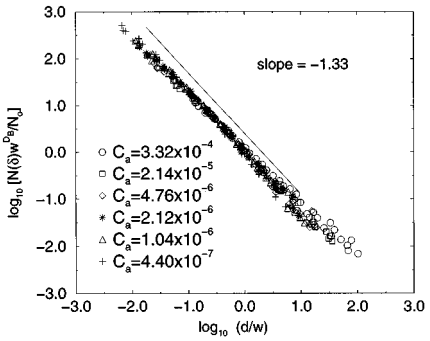


FIG. 5. Data collapse of the box counting data of the fronts for six experiments. The box dimension was found to be $D_b = 1.33 \pm 0.05$.

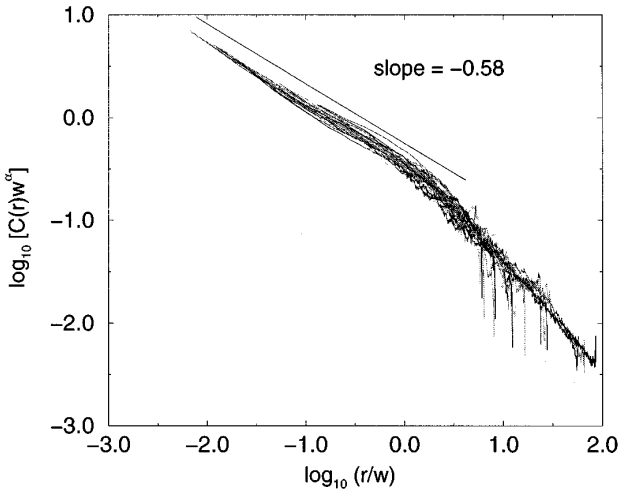


FIG. 6. The density-density correlation function data of the front for experiments with $C_a = 3.32 \times 10^{-4}$, $2.14 \times 10^{-5}$, $4.76 \times 10^{-6}$, $2.12 \times 10^{-6}$, $1.04 \times 10^{-6}$, and $4.40 \times 10^{-7}$. The fractal dimension $D_d$ was found to be $D_d = 1.42 \pm 0.05$.

with a growth zone restricted to the hull [27], the fractal dimension of the cluster is found to be $D = 1.86 - 1.89$ [15,27], while if the growth zone is restricted to the external perimeter it is $D = 1.83$ [8,25,26,28]. By using this result in Eq. (6) we find $\tau = 1.92$ with a growth zone restricted to the external perimeter, and $\tau = 1.93 - 1.95$ with a growth zone restricted to the hull.

The exponent $\tau$ estimated from the cumulative cluster size distribution is found slightly lower than the theoretical estimate given by Meakin [28]. We attribute this discrepancy to finite-size corrections that we expect to be large since his argument relies on the divergence of a term $s^{2-\tau}$ when $s \to \infty$. This divergence is very slow, as $2 - \tau$ is barely positive, and as a result, the asymptotic scaling regime is only reached for very large systems. Since our result is within three standard deviations of the result of invasion percolation, we cannot conclude that our result is inconsistent with

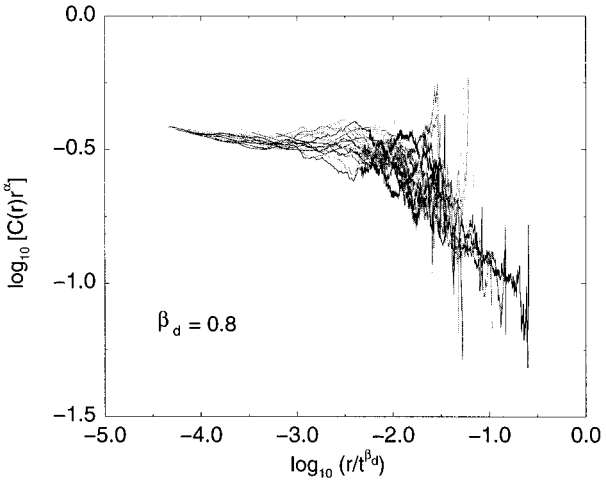


FIG. 7. The dependence of $C(r)r^{\alpha}$ on $r/t^{\beta_d}$ with $\beta_d = 0.8$ giving the best data collapse. Arbitrary units have been used. The capillary number was $C_a = 4.40 \times 10^{-7}$.

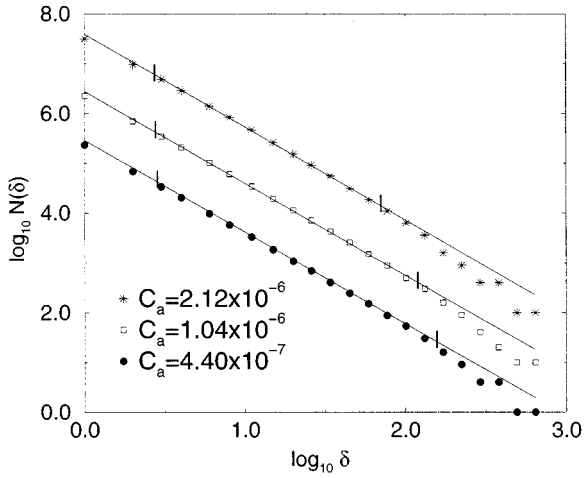


FIG. 8. The dependence of the number of boxes $N(\delta)$ needed to cover the front as a function of $\delta$ for three slow experiments. The box counting dimension estimated from the slope of the curves is $D_b^m = 1.85 \pm 0.10$. The slopes were fitted to the points between the vertical marks indicating the pore size and the largest trapped clusters. The experiments with $C_a = 1.04 \times 10^{-6}$ and $C_a = 2.12 \times 10^{-6}$ were shifted, respectively, $+1.0$ and $+2.0$ along the $y$ axis for a better view. Here, $\delta$ is measured in units of pixel size, and 1 pixel $= 0.21$ mm.

what is expected from invasion percolation with trapping.

## IV. DISCUSSION

We have performed drainage experiments in a two-dimensional porous medium. The main focus of the work is the study of the structure and dynamics of the front for different flow rates when both fluids have the same viscosity. From the experiments we clearly see a stabilizing effect on the front at high injection rates. The stabilizing effect is due to a lower effective permeability $K_{\text{eff}}$ in the injected fluid than in the displaced fluid. The lower effective permeability

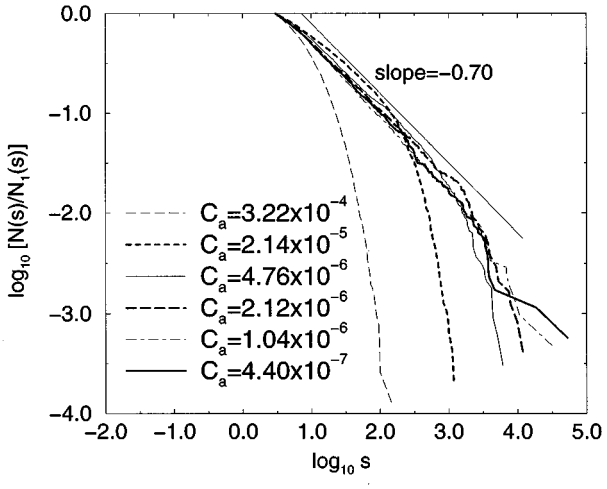


FIG. 9. The normalized cumulative cluster size distribution for six experiments. The slope of the line is $-0.70$, giving a value of $\tau = 1.70 \pm 0.10$. Here, $s$ is measured in units of pixel area, i.e., 1 pixel area equals 0.21 mm $\times$ 0.21 mm.

results from the trapping and flow in local capillary fingers. Trapping reduces the total pore volume accessible to the invaded fluid. This implies a decrease in the effective permeability $K_{\text{eff}}$ of the invaded regions. The capillary fingers of the invaded fluid are more narrow than the fjords of the displaced fluid, as can be seen in Fig. 3. This implies an even further reduction in the permeability of the invaded regions. The stabilizing effect may be seen through noting that it is the mobility $K_{\text{eff}}/\mu$ which enters the Darcy equation. A *decrease* in effective permeability may just as well be interpreted as an *increase* in effective dynamic viscosity — and thus we are effectively dealing with a more viscous liquid displacing a less viscous liquid, which leads to a stable front.

In order to develop more precisely the argument just presented, we argue as follows: The lower effective permeability in the injected liquid increases the absolute value of the pressure gradient in this liquid compared with the absolute value of the pressure gradient in the displaced liquid. As a rough estimate, consider $dp_i/dx$ to be an average pressure gradient in the injected fluid and $dp_d/dx$ to be an average pressure gradient in the displaced fluid. Here the positive $x$ direction is chosen in the direction of the average flow. Furthermore, let $l$ be the distance in the direction of the flow between two points $A$ and $B$. Here $A$ and $B$ are chosen as two points on the front and $A$ is downstream compared with $B$. The pressure drop going from $B$ (at the injected fluid side) to $A$ (at the displaced fluid side) through the injected fluid equals the pressure drop going from $B$ to $A$ through the displaced fluid. This gives the balance equation

$$l\frac{dp_i}{dx} - \Delta p_A = l\frac{dp_d}{dx} - \Delta p_B \tag{7}$$

for the pressure. Let us now compare the difference in the capillary pressure given by Eq. (7) with the width of the capillary pressure threshold distribution. The pressure threshold distribution is only a function of the interfacial tension, the wetting properties, and the distribution of the pore sizes in the system, i.e., a purely local quantity. Assume that the width of the pressure threshold distribution is equal to $c\gamma/a$, where $c$ is a dimensionless constant. The width $w = l$ of the front must then be apparent when $c\gamma/a$ is equal to the capillary pressure difference $\Delta p_B - \Delta p_A$. This is when

$$\Delta p_B - \Delta p_A = w\left(\frac{dp_d}{dx} - \frac{dp_i}{dx}\right) = c\frac{\gamma}{a}. \tag{8}$$

Thus, since the term $dp_d/dx - dp_i/dx$ is positive, and increases with a lower effective permeability of the injected fluid, this stabilizes the front.

The front was found to be fractal with a fractal dimension $D_b = 1.33$, consistent with the fractal dimension of the external perimeter of invasion percolation. By measuring the fractal dimension of the structure left behind the front we found a fractal dimension $D_b^m = 1.85$ also consistent with the results of invasion percolation with trapping. We emphasize that

these results were also found when the structure was stabilized, but on a length scale smaller than the width of the front.

The dynamic exponent $\beta_d = 0.8 \pm 0.3$, found by collapsing the density-density correlation function, is uncertain, due to the finite size of our models. To improve these results, experiments need to be done on models much larger than ours.

**ACKNOWLEDGMENTS**

The authors thank E. Aker, S. Basak, G.G. Batrouni, J. Feder, E.G. Flekkøy, V. Frette, L. Furuberg, R. Lenormand, and S. Roux for valuable comments. The work was supported by NFR, the Norwegian Research Council, and the CNRS through a PICS grant.

[1] K.J. Måløy, J. Feder, and T. Jøssang, Phys. Rev. Lett. **55**, 2688 (1985).
[2] J.D. Chen and D. Wilkinson, Phys. Rev. Lett. **55**, 1892 (1985).
[3] R. Lenormand, E. Touboul, and C. Zarcone, J. Fluid Mech. **189**, 165 (1988).
[4] M. Cieplak and M.O. Robbins, Phys. Rev. Lett. **60**, 2042 (1988).
[5] M. Cieplak and M.O. Robbins, Phys. Rev. B **41**, 11 508 (1990).
[6] N. Martys, M. Cieplak, and M.O. Robbins, Phys. Rev. Lett. **66**, 1058 (1991).
[7] P.G. de Gennes and E. Guyon, J. Mech. **17**, 403 (1978).
[8] D. Wilkinson and J.F. Willemsen, J. Phys. A **16**, 3365 (1983).
[9] R. Lenormand and C. Zarcone, Phys. Rev. Lett. **54**, 54 (1985).
[10] A. Birovljev, L. Furuberg, J. Feder, T. Jøssang, K.J. Måløy, and A. Aharony, Phys. Rev. Lett. **67**, 584 (1991).
[11] V. Frette, J. Feder, T. Jøssang, and P. Meakin, Phys. Rev. Lett. **68**, 3164 (1992).
[12] P. Meakin, J. Feder, V. Frette, and T. Jøssang, Phys. Rev. A **46**, 3357 (1992).
[13] W.B. Haines, J. Agric. Sci. **97**, 97 (1930).
[14] L. Furuberg, J. Feder, A. Aharony, and T. Jøssang, Phys. Rev. Lett. **61**, 2117 (1988).
[15] S. Roux and E. Guyon, J. Phys. A **22**, 3693 (1989).
[16] K.J. Måløy, L. Furuberg, J. Feder, and T. Jøssang, Phys. Rev. Lett. **68**, 2161 (1992).
[17] S. Maslov, Phys. Rev. Lett. **74**, 562 (1995).
[18] L. Furuberg, K.J. Måløy, and J. Feder, Phys. Rev. E **53**, 966 (1996).
[19] K.J. Måløy, F. Boger, J. Feder, T. Jøssang, and P. Meakin, Phys. Rev. E **36**, 318 (1987).
[20] U. Oxaal, M. Murat, F. Boger, A. Aharohny, J. Feder, and T. Jøssang, Nature **329**, 32 (1987).
[21] D. Wilkinson, Phys. Rev. A **30**, 520 (1984).
[22] D. Wilkinson, Phys. Rev. A **34**, 1380 (1986).
[23] K. Hansen, J. Colloid Interface Sci. **160**, 209 (1993).
[24] J. F. Gouyet, M. Rosso, and B. Sapoval, Phys. Rev. B **37**, 1832 (1988); M. Rosso, J. F. Gouyet, and B. Sapoval, Phys. Rev. Lett. **57**, 3195 (1986).
[25] T. Grossman and A. Aharony, J. Phys. A **19**, L745 (1986).
[26] T. Grossman and A. Aharony, J. Phys. A **20**, L1193 (1986).
[27] R.F. Voss, J. Phys. A **17**, L373 (1984).
[28] P. Meakin, Physica A **173**, 305 (1991).